THE DESIGN OF A MULTI-BEAM ELECTRON GUN FOR A PHOTONIC FREE-ELECTRON LASER*

J.H.H. Lee#, T. Denis, P.J.M. van der Slot, K.J. Boller, University of Twente, MESA+ Institute for Nanotechnology, Enschede 7500AE, The Netherlands.

Abstract

The photonic Free-Electron Laser (pFEL) is a novel slow-wave device which relies on a photonic crystal (PhC) to synchronize an electromagnetic wave with co-propagating electron beams [1-3]. The advantage of a pFEL is in its frequency- and power-scaling properties. The scale invariance of Maxwell's equations allows the use of the same beam energy to operate at higher frequencies when the PhC is correspondingly scaled. Meanwhile, power-scaling is achieved by varying the number of electron beams propagating in parallel through the PhC. To produce a set of parallel beams, we have designed a multi-beam electron gun using flat cathodes, which produces a total current of 1 A at a beam voltage of 14 kV. We will present the design of this gun together with the achievable performance. In addition, we have investigated the beam transport system and will discuss the options for guiding the beams through the PhC.

INTRODUCTION

As a slow-wave device, the pFEL operates whence the phase velocity of radiation is less than the velocity of charged particles. However, unlike other slow-wave devices, the pFEL is capable of generating relatively high output power at high frequencies, e.g., THz. This is realized by increasing the interaction volume (i.e., number of parallel electron beams) while maintaining fully coherent output. The other advantage of utilizing a multi-beam configuration is that lower gun perveance from each beam allows for higher efficiency while attaining a high total perveance for the device.

The experimental demonstration of power scaling and the study on the development of coherence in the pFEL requires individual beam switching, i.e., each individual beam can be independently switched on or off. One method to realize this is to use individual emitters as sources for the electron beams.

Here, we started with the planar space-charged limited Pierce gun with rectilinear flow [4], and subsequently improve the geometry based on design requirements such as the mechanical structure of the emitter, beam modulation requirements, and so on. Corrections are then made to compensate for the non-linearities introduced by these alterations from the ideal gun. For beam transport, immersed flow or confined flow is adopted considering its beneficial properties for the pFEL.

This paper discusses the design of a single gun from careful shaping of the electrodes and correctly applied voltages to an integrated multi-beam gun providing parallel beams with excellent beam quality in terms of laminarity, transverse emittance, axial velocity spread and brightness.

*Work supported bythe Dutch Technology Foundation STW, applied science division of NWO and the technology program of the Ministry of Economic Affairs

#j.h.h.lee@utwente.nl

SINGLE-BEAM GUN DESIGN

An impregnated cathode with a diameter of 1 mm and maximum current density of 8 A/cm^2 from LG-Philips has been considered for our gun design. As with any thermionic cathode, the gun will operate under space-charged limited emission to obtain good beam uniformity. We will first start with the gun design methodology and then continue with the design progression of the gun. The optimal single-beam gun design will be proliferated into a multi-beam gun design in the next section, where we investigate the mutual coupling between the beams.

Gun Design Methodology

The finite element solver Opera 3D SCALA from Vector Field is used to solve the electrostatic Poisson's equations for the charged particles in the gun with given boundary conditions. As a start, Child's law particle emission model is employed to create the beam. In a follow-up study the Langmuir/Fry (LF) emission model will be used. The difference between the two models is the former assumes zero initial energy particles while the latter includes non-zero initial energy with one-dimensional Maxwell distribution.

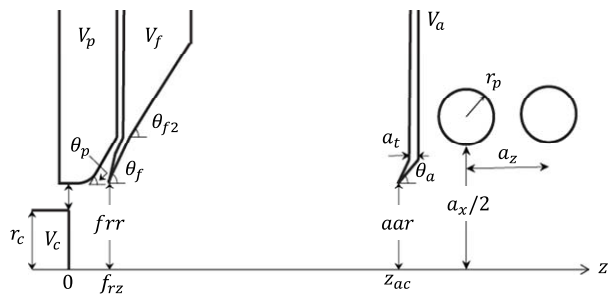

Figure 1: Geometry and parameters of the gun design incorporating PhC and waveguide.

The single-beam gun geometry is shown in Figure 1 together with the definition of several geometry parameters and voltages. Also shown is an example of a photonic structure that starts behind the anode. Considering the cathode-anode distance, z_{ac}, is much larger than the cathode radius, r_c, we can assume the effect of the anode aperture to have negligible effect in the cathode region. Thereby, we can design the electrodes

ISBN 978-3-95450-117-5

in the cathode region independent of the anode. Likewise for the anode, we can independently shape the electrode to minimize the distortion due to the anode aperture, with beam emission from an ideal Pierce gun.

An important feature desired of the multi-beam gun is independent beam switching. Cathode pulsing is employed where the cathode voltage is toggled to switch the respective beam on-and-off. This has the added benefit of a constant field between the focus electrode and the anode compared to the focus electrode pulsing. To obtain a low switching voltage swing between on-off states, the focus electrode is then placed close to the cathode and at the same time the radius of focus electrode aperture, *frr*, is kept small. The strategy is to have a fixed radius of aperture (1.2**rc*) just large enough for the beam to pass through without being intercepted, and then optimize the distance between the focus electrode and the cathode for the lowest possible switching voltage. This distance has been found to be around 0.2 mm from the cathode emission surface. However, low switching voltage will compromise beam quality. Hence, careful design considerations have to be taken near the cathode region.

There are inherent advantages of using low and zero compression guns as they are consistent with good beam quality and lower tolerance sensitivity [5]. In terms of cost and ease of design, we are using flat surface emission emitters and immersed flow for the initial design of the multi-beam gun.

Definitions of Beam Properties

Emittance [6] is a measure of the parallelism of the beam - laminarity. The equation for normalized rms emittance from [7]

$$\varepsilon_{\mathrm{n,x,rms}} = \frac{1}{m_0 c}\sqrt{\langle x^2\rangle\langle p_x^2\rangle - \langle x p_x\rangle^2} \qquad \text{m-rad} \quad (1)$$

is adopted since the second central moment is used, which means that the emittance is irrespective of shift in reference position as this will be useful for the case of the multi-beam configuration. We will only consider the transverse emittances $\varepsilon_{\mathrm{n,x,rms}}$ and $\varepsilon_{\mathrm{n,y,rms}}$.

The axial velocity spread is calculated using the normalized current weighted standard deviation,

$$\frac{\Delta \mathrm{v_z}}{\overline{v_z}} = \frac{\sqrt{\sum I_i \left(v_z - \overline{v_z}\right)^2}}{\overline{v_z}} \quad (2)$$

$$\text{where} \quad \overline{v_z} = \frac{\sum I_i v_{zi}}{\sum I_i} \,. \quad (3)$$

Besides that, beam brightness [6] is useful as it gives a measure of both good beam laminarity and high current density. The normalized brightness is specified as

$$\mathrm{B_n} = \frac{I}{\pi^2 \varepsilon_{n,x,rms}\varepsilon_{n,y,rms}} \ \mathrm{A/m^2\text{-}rad^2}. \quad (4)$$

Pierce Electrode

For the gun, the Pierce electrode with 67.5° angle to the beam to sustain a finite laminar beam needs to be modified for cathode fitting, and thermal isolation. Aside from that, the separation gap between the cathode and Pierce electrode must meet the limit for maximum electric field breakdown. Assuming the allowed maximum electric field is 2.4 MV/m and the maximum voltage between the two electrodes to be 350 V, a minimum separation about 150 μm is required. The introduction of the separation gap degrades the emittance and axial velocity spread. Both of these beam properties increases by 50% and 36% respectively, as the separation gap increases to 150 μm.

The modified Pierce electrode is shaped following the equipotential layout of a rectilinear beam gun [4]. From observation, smaller θ_p and more negative V_p are required when a separation gap is introduced. As the Pierce electrode is a distance away from the cathode, sufficient negative potential V_p is required to suppress the cathode edge emission and also keeping the radial force balanced.

Focus Electrode

As mentioned earlier, a focus electrode close to the cathode is desired in order to obtain a low beam switching loss. In addition, the focus electrode also plays a role in beam focusing and control. The ideal focus electrode should be very thin following the equipotential lines for a rectilinear flow. However, this is not practical since a reasonably thick electrode is required for mechanical reliability and robustness. Also, a sufficiently thick electrode is necessary to induce an electrostatic field dampener to allow for a low switching voltage.

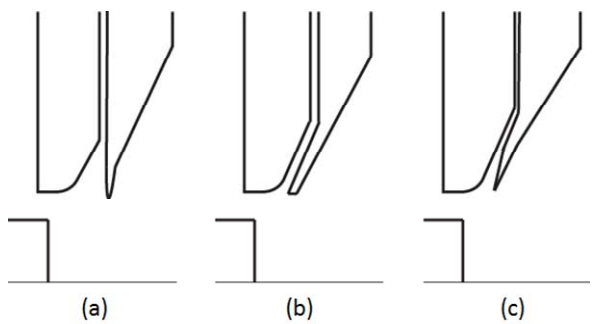

Figure 2: Shaping of the focus electrode with the modified Pierce electrode.

A selection of various electrode shapes has been investigated (See Figure 2). The configuration of choice is Figure 2 (c). It allows for a low switching voltage of 350 V and a better mapping to the equipotential of a rectilinear flow. This region near the surface emission is very critical as the kinetic energy is very low. Therefore, intensive tuning and iterations are performed to achieve the best possible beam quality.

ISBN 978-3-95450-117-5

Anode

Similar to other electrodes, shaping of anode has been carried out to correct the field distortion caused by the anode aperture. Straight electrode is preferred rather than tilted or curved for two reasons. Firstly, it is observed for this case that straight electrode gives better beam quality. Secondly, the backside of the electrode will act as a mirror for the radiation wave generated in the photonic structure. After several iterations, the best correction is given by the anode with an extended tip and low effective thickness as in Figure 3 (d). Also, a converging beam near the anode aperture will help improve beam quality by countering the diverging effect of the aperture.

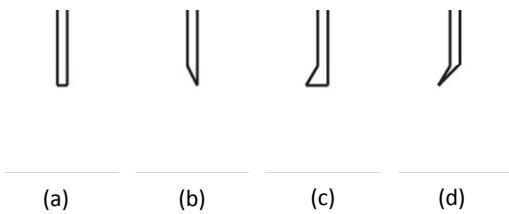

Figure 3: Shaping of the anode tips with straight electrode.

Beam Transport

For the immersed flow, electrons are tied to the field lines, ensuring good beam parallelism hence better beam control and ease of design compared to the Brillouin flow. Even though it is possible in theory to obtain a ripple-free beam using the Brillouin flow, much higher B_z is usually required and the precessional angular velocity in immersed flow is about 1/10 of the rotational Larmor angular velocity in the Brillouin flow [8]. Moreover, immersed flow is more suitable for annular beam transport [8], which supports higher current limit, and possibly higher pFEL efficiency compared to the solid cylindrical beam. However, if higher compression guns or lower magnetic fields are required, Brillouin flow is then the preferred choice for beam transport with the exception of very high current beams [6].

Immersed flow requires that the gun be submerged in a magnetic field, B_z. High magnetic field strength is required to achieve high beam parallelism. From simulation result, the degree of envelope oscillation is a function of the normalized initial slope, and the magnetic field and space-charge parameter as noted in [8]. If the beam transverse velocity is made small, good parallelism and minimal ripples can be achieved with lower magnetic strength. The calculated magnetic field value required for envelope oscillation of less than 10% of the beam radius is approximately 0.1 T. However, simulation results show that at least 0.2 T is required.

Envelope oscillation of the beam is inherent for beam transport utilizing immersed field, thereby beam properties like emittance will tend to oscillate along the propagation distance. This is apparent after the anode aperture. The emittance is at its minima when transitioning between the maximum and minimum beam radii, while minima at the zero derivative points (see Figure 4). As for the axial velocity spread, it starts out high after being emitted from the cathode, gradually improve until it gave a sudden jump at the anode aperture and continue to decrease to very low values. Figure 5 shows the plots for the emittance and axial velocity spread, and the beam trajectories for B_z = 0.4 T.

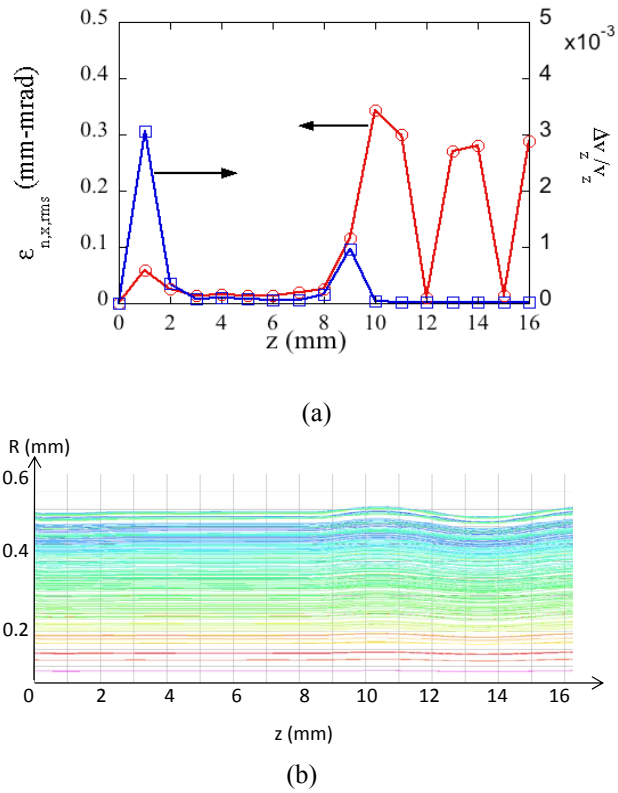

Figure 4: Beam parameters (a) and electron trajectories (b) for the single-beam gun.

It has been observed that guided beams that converge at the anode aperture give higher maximum beam quality than otherwise. We also notice the precession of electrons besides their cyclic variation in angle and radius as discussed in [8]. The beam distribution in phase space tends to behave more ellipsoidal in the applied magnetic field.

MULTI-BEAM GUN DESIGN

In this section, we will construct a linear multi-beam as in Figure 5 using the single-beam gun design derived in the previous section with gun parameters as shown in Table 1. From the table, current emission for a single emitter is 30 mA as a result of electrode shaping in the cathode region. This can be easily increase to 50-60 mA by reducing the anode-cathode distance, z_{ac} to 6 mm. To obtain a total current of 1 A, a total number of at least 20 beams are required. Here we investigate a linear array, and the electrostatic coupling between the beams. This information can be also used to construct two-

ISBN 978-3-95450-117-5

dimensional arrays, which leads to more compact electron guns.

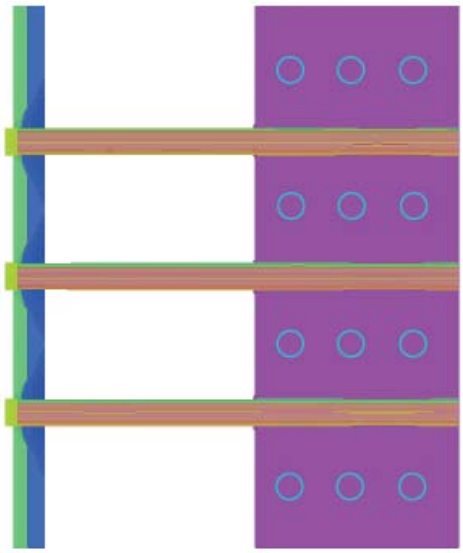

Figure 5: Multi-beam gun configuration with a PhC.

Table 1: Gun Parameters of a Single-beam Gun

I	30 mA	f_{rz}	0.2 mm
V_p	-36 V	z_{ac}	8.78 mm
V_f	60 V	θ_p	66°
V_a	14 kV	θ_f	80°
frr=aar	0.6 mm	θ_{f2}	65°

The minimum beam-to-beam spacing is 5 mm, which is constrained by the size of the chosen discrete emitter. When the beam-to-beam distance is varied, the simulations show that changes in transverse emittance and axial velocity spread are small and the individual beam characteristics are very close to those of the single-beam gun (see Figure 4). The rms normalized emittance $\varepsilon_{n,x,rms}$ is shown together with the rms axial velocity spread in Figure 6 at a position 16 mm from the cathode (i.e., a about 7 mm behind the anode aperture). Note, the low axial velocity spread is due to Child's emission model, resulting from emission with zero velocity spread. A more realistic emission model that includes an initial velocity spread will produce more realistic values. The results here show that the optimized gun geometry does not introduce much axial velocity spread, both for the single- and multi-beam versions.

The results obtained here suggest that, from a beam point of view, a more dense packing than the minimum imposed by our choice of discrete emitter is possible. We will further verify this with a more realistic cathode emission model that includes initial velocity spread.

The choice of one- or two-dimensional arrays (i.e., symmetries present in the electron beam) may also be influenced by space-charge depression at the entrance to the collector [9].

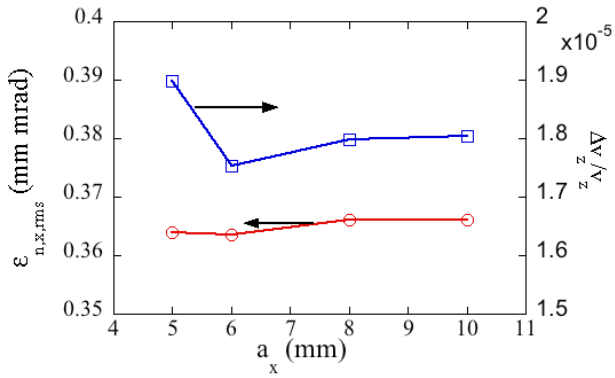

Figure 6: Effect of beam-to-beam spacing on beam properties at a position of 16 mm from the cathode.

CONCLUSION

A single-beam gun utilizing discrete flat emission surface emitter has been optimized to produce a good quality electron beam assuming Child's law as cathode emission model. The single-beam geometry is then used to construct a multi-beam gun, which can be used as electron source for a photonic free-electron laser. It is found that the individual beams do not affect each other for the range of beam spacing investigated. The single emitter can produce a maximum of ~50 mA, so an array of 20 beams is required to produce a total beam current of 1 A. Immersed flow has been used for beam transport. Further studies will be carried out with (i) a more realistic cathode emission model that includes initial velocity spread and (ii) the immersed flow will be compared with Brillouin flow to obtain a multi-beam electron gun with optimum beam parameters.

REFERENCES

[1] E. Jerby, A. Kesar, M. Korol, L. Lei, and V. Dikhtyar IEEE Trans. Plasma Sc. **27**, 445 (1999).
[2] P.J.M. van der Slot, T. Denis, K.J. Boller, Proceedings of the 30th international FEL conference, p. 231 (2008).
[3] V.G. Baryshevsky, Nucl. Instrum. Methods Phys. Res. A**445**, 281 (2000).
[4] J. R. Pierce, J. Appl. Phys., **11**, 548 (1940)
[5] M. Read, L. Ives, T. Bui, and H. Tran, 2010 IEEE International Vacuum Electronics Conference, 75 (2010).
[6] S. Humphries, *Charged Particle Beams*, Wiley-Interscience, 1990.
[7] K. Floettmann, Phys Rev. STAB **6**, 034202 (2003).
[8] G. R. Brewer, IRE Trans. Electr. Devices, **4**, 134 (1957).
[9] K. T. Nguyen, D. E. Pershing, D. K. Abe, G. Miram, and B. Levush, IEEE Trans. Plasma Sc., **33**, 685 (2005).

ISBN 978-3-95450-117-5